

Temperature–Pressure Phase Diagram of a D<sub>2</sub>O–D<sub>2</sub> System at Pressures to 1.8 kbarVadim S. Efimchenko,<sup>\*,†</sup> Vladimir E. Antonov,<sup>†</sup> Oleg I. Barkalov,<sup>†</sup> and Semen N. Klyamkin<sup>‡</sup>*Institute of Solid State Physics, Russian Academy of Sciences, 142432 Chernogolovka, Moscow District, Russia, and Department of Chemistry, Moscow State University, 119991 Moscow, Russia**Received: January 17, 2008; In Final Form: March 24, 2008*

Using a volumetric technique, the deuterium solubility,  $X$ , in heavy water (L), low-pressure hexagonal ice (I<sub>h</sub>), and high-pressure cubic clathrate ice (sII) is studied at deuterium pressures up to 1.8 kbar and temperatures from  $-40$  to  $+5$  °C. The triple point of the L + I<sub>h</sub> + sII equilibrium is located at  $P = 1.07(3)$  kbar and  $T = -4.5(8)$  °C. The molar ratios D<sub>2</sub>/D<sub>2</sub>O of phases at the triple point are  $X_L = 0.020(5)$ ,  $X_{I_h} = 0.012(5)$ , and  $X_{sII} = 0.207(5)$ .

**Introduction**

Phase transformations in the water–hydrogen system have recently attracted close attention due to the discovery of new hydrogen clathrate hydrate.<sup>1–3</sup> The cubic unit cell of the sII-type<sup>2</sup> crystal structure of this clathrate phase is composed of 136 H<sub>2</sub>O molecules and can accommodate from 27.2<sup>4</sup> to 48<sup>3</sup> guest molecules of H<sub>2</sub>, which gives a molar ratio of H<sub>2</sub>/H<sub>2</sub>O = 0.200–0.353. The clathrate with these compositions is formed at hydrogen pressures of 1–3.6 kbar.<sup>1</sup> If quenched under high pressure, the clathrate is metastable in vacuum at temperatures up to 145 K.<sup>2</sup> The rather high hydrogen capacity makes the sII clathrate a promising candidate for hydrogen storage applications.<sup>2,5</sup> The clathrate is of significant interest for planetary science and astrophysics because its formation pressure is low enough to be reached inside small icy satellites and because hydrogen trapped in interstellar ices can be in the form of this clathrate due to its thermal stability at low pressure.<sup>2</sup>

Some significant properties of the hydrogen clathrate hydrate, such as the crystal structure,<sup>3</sup> the maximum<sup>3</sup> and minimum<sup>4</sup> concentrations of the guest hydrogen molecules, and the formation kinetics,<sup>3</sup> were studied by neutron diffraction on deuterium-substituted D<sub>2</sub>O–D<sub>2</sub> samples. At the same time, the temperature–pressure ( $T$ – $P$ ) phase diagram of the D<sub>2</sub>O–D<sub>2</sub> system has never been examined. In the present paper, we construct the lines of phase transitions between the liquid phase (L), low-pressure hexagonal ice (I<sub>h</sub>), and clathrate phase (sII) and determine the deuterium content of these phases in the vicinity of the L–I<sub>h</sub>–sII triple point in the D<sub>2</sub>O–D<sub>2</sub> system using a volumetric technique. The feasibility of the obtained data was additionally tested and improved by comparing with earlier results for the H<sub>2</sub>O–H<sub>2</sub> system.<sup>4,6</sup>

**Experimental Details**

The experimental setup is described in ref 7. The measurements were carried out in an atmosphere of molecular deuterium taken in excess. The D<sub>2</sub> gas with isotopic purity 99.9% was prepared by thermal decomposition of a LaNi<sub>5</sub>-based deuteride. The heavy water had an atomic ratio of H/D = 10<sup>–3</sup>.

The amount of deuterium absorbed by the sample was determined volumetrically from the pressure and temperature

in the calibrated volume of the measuring system. The molar ratio  $X = D_2/D_2O$  of the absorbed deuterium was calculated with an accuracy of  $\pm 0.005$  by using published data on the pressure and temperature dependences of the molar volumes of deuterium-substituted liquid water and ice, I<sub>h</sub>,<sup>8</sup> the sII phase<sup>2–4</sup> and gaseous deuterium.<sup>9</sup> The solubility of water in gaseous hydrogen was earlier shown to be vanishingly small at 27 °C and pressures up to 6 kbar,<sup>10</sup> so we neglected the solubility of heavy water in the deuterium gas in our experiments at pressures up to 1.8 kbar. The deuterium dissolved in heavy water and ice I<sub>h</sub> was assumed to increase their molar volumes by the same value of  $\partial V/\partial X = 7.95$  cm<sup>3</sup>/mol as hydrogen dissolved in liquid H<sub>2</sub>O. The adopted  $\partial V/\partial X$  value is the average of experimental results of refs 11 and 12.

Each studied sample of D<sub>2</sub>O weighing  $\sim 1.5$  g was frozen and powdered in an agate mortar under liquid nitrogen prior to the high-pressure experiment to speed up the kinetics of deuterium absorption and desorption. Changing the temperature or the total hydrogen amount in the autoclave led to a temporal drift of the pressure. The drift lasted  $\sim 5$ – $3$  min in the absence of phase transitions;  $\sim 1$  h in the course of the I<sub>h</sub>  $\rightarrow$  sII and sII  $\rightarrow$  I<sub>h</sub> transitions;  $\sim 5$  min when the I<sub>h</sub> phase was melted or crystallized;  $\sim 5$  min when the sII phase was crystallized, and  $\sim 20$  min when it was melted. While constructing isotherms or isochors, the closed autoclave was held at every point at fixed temperature until the pressure stopped changing. The pressure was measured accurately to  $\pm 3$  bar. The temperature was determined with an accuracy of  $\pm 0.1$  °C and could be kept constant within  $\pm 0.3$  °C.

**Results and Discussion**

The constructed  $T$ – $P$  diagram of phase equilibria in the D<sub>2</sub>O–D<sub>2</sub> system is shown as thick solid lines in Figure 1. The lines of the I<sub>h</sub>  $\leftrightarrow$  L and sII  $\leftrightarrow$  L equilibria are drawn through the experimental melting points of the I<sub>h</sub> and sII phase, correspondingly, because the equilibrium line is always much closer to the melting curve than to the curve of crystallization. The line of the I<sub>h</sub>  $\leftrightarrow$  sII equilibrium is plotted in the middle between the points of formation (solid circles) and decomposition (open circles) of the sII phase.

The L  $\rightarrow$  sII transition that occurred on cooling the liquid (solid squares in Figure 1) was incomplete, and the samples were composed of mixture of the I<sub>h</sub> and sII phases. Further heating of these samples allowed construction of a metastable

\* To whom correspondence should be addressed. E-mail: efimchen@issp.ac.ru.

<sup>†</sup> Institute of Solid State Physics, Russian Academy of Sciences.

<sup>‡</sup> Department of Chemistry, Moscow State University.

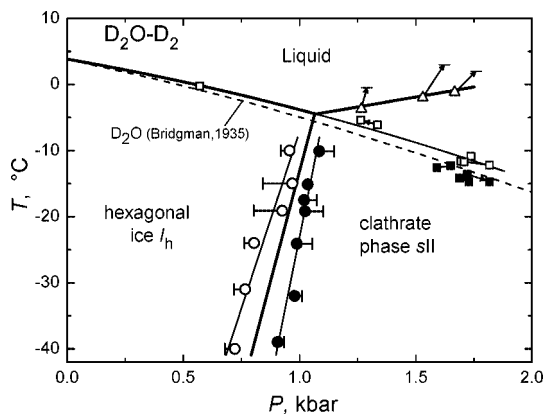


**Figure 1.**  $T$ - $P$  phase diagram of the D<sub>2</sub>O–D<sub>2</sub> system. Pairs of a solid circle and a vertical bar connected with a horizontal line indicate the minimum and maximum pressures of the I<sub>h</sub> → sII transition at increasing pressure. Similar pairs with open circles show the maximum and minimum pressures of the reverse sII → I<sub>h</sub> transition. The thick solid line plotted in the middle between the solid and open circles represents the I<sub>h</sub> ↔ sII equilibrium. Pairs of an open triangle and a horizontal bar connected with an arrow indicate the starting and finishing points of melting of the sII phase at increasing temperature. The solid line representing the sII ↔ L equilibrium is plotted through the starting points (see text). Pairs of open and solid squares show, respectively, the intervals of melting and crystallization of ice I<sub>h</sub>. The curve of the I<sub>h</sub> ↔ L equilibrium is drawn through the melting points. Its stable part is shown by the thick solid curve and the metastable extension beyond the L + I<sub>h</sub> + sII triple point by the thin solid curve. The dashed line shows the melting temperature of D<sub>2</sub>O ice I<sub>h</sub> in the absence of gaseous deuterium.<sup>8</sup>

prolongation of the melting line of the I<sub>h</sub> phase (thin solid line drawn through the open squares) into the stability region of the sII phase. As seen from Figure 1, the melting curve of heavy ice I<sub>h</sub> in a deuterium atmosphere slightly deviates from that in the absence of deuterium (the dashed line<sup>8</sup>) as the pressure increases, but the effect does not exceed 2 °C at 1.8 kbar.

The I<sub>h</sub>, sII, and L phases coexist at equilibrium at 1.07(3) kbar and –4.5(1) °C. Formally, this is a quadruple point because the three condensed phases are also at equilibrium with the gaseous H<sub>2</sub> phase. However, as long as the gaseous phase is in excess and undergoes no phase transitions, its occurrence decreases the variance of the condensed system exactly by 1. Considered separately from the gaseous phase, the condensed system therefore obeys the reduced phase rule, and the topology of its  $T$ - $P$  phase diagram should be that of a one-component system. In particular, no two-phase regions are possible: two condensed phases can coexist only along lines, and three phases coexist only at isolated points. The deuterium concentration of each condensed phase is a sort of an internal parameter determined by the gas temperature and pressure in a unique fashion. It is standard practice to count only condensed phases in the metal–hydrogen systems, and we believe this approach is worth being adopted for the water–hydrogen system, too, because it simplifies the analysis of the diagram. The point of the L + I<sub>h</sub> + sII equilibrium is therefore called a triple point in the present paper.

The molar ratios D<sub>2</sub>/D<sub>2</sub>O of phases at the triple point are  $X_L = 0.020(5)$ ,  $X_{I_h} = 0.012(5)$ , and  $X_{sII} = 0.207(5)$ . The indicated error refers to the absolute values of deuterium solubilities in the condensed phases. The difference  $X_L - X_{I_h} = 0.008(4)$  was determined with a better accuracy, and it is definitely positive.

Below, we will discuss in more detail the experimental results used to construct the  $T$ - $P$  diagram of Figure 1 and to determine the compositions of phases at the triple point.

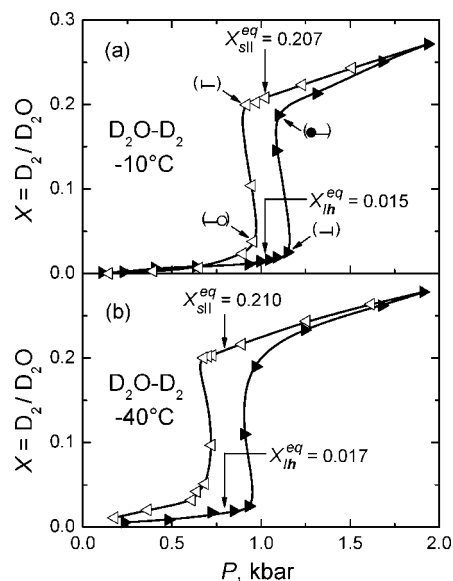


**Figure 2.** Isotherms of deuterium solubility in D<sub>2</sub>O ices at –10 and –40 °C. Solid and open triangles refer to increasing and decreasing pressure, respectively. Arrows near the bracketed symbols indicate the positions of the corresponding symbols in Figure 1.

**The I<sub>h</sub> ↔ sII Transformation.** Typical isotherms of deuterium solubility used to determine the points of the I<sub>h</sub> → sII and sII → I<sub>h</sub> transitions are shown in Figure 2.

As one can see from Figure 2a, the deuterium solubility in the low-pressure ice, I<sub>h</sub>, at –10 °C monotonically grows with pressure and reaches a molar ratio, D<sub>2</sub>/D<sub>2</sub>O, of  $X \approx 0.02$  at  $P = 1.1$  kbar. In a narrow pressure interval of 1.1–1.15 kbar, the solubility rises by an order of magnitude, signaling the transformation to the clathrate phase, sII. Further increase in pressure leads to a monotonic increase in the solubility up to  $X \approx 0.27$  at  $P = 1.94$  kbar. The subsequent decrease in pressure is accompanied by a gradual descent of the deuterium solubility in the sII phase down to  $X \approx 0.20$  at  $P = 0.92$  kbar with the following steep decrease to  $X \approx 0.02$  due to the reverse sII → I<sub>h</sub> transition.

The  $X(P)$  isotherms measured at other temperatures look similar to those at –10 °C and demonstrate a clear baric hysteresis of the I<sub>h</sub> ↔ sII transformation. Another common feature of all isotherms is that they are S-shaped in the intervals of the I<sub>h</sub> → sII and sII → I<sub>h</sub> transitions. These effects are typical of hydrate formation and decomposition in water–gas systems (see, e.g., ref 13 and references therein) and are due to the fact that both transitions include processes of nucleation and growth of a new phase, and the nucleation is fast and abundant. Each process requires a thermodynamic driving force to proceed. In our case, this driving force is the Gibbs energy,

$$\Delta G = \int_{P_{eq}}^P \Delta V dP$$

where  $\Delta V$  is the volume effect of the I<sub>h</sub> → sII or sII → I<sub>h</sub> transition, and  $P_{eq}$  is the equilibrium pressure of the I<sub>h</sub> ↔ sII transformation.

The driving force,  $\Delta G_n$ , necessary for the nucleation is larger than  $\Delta G_g$  for the growth process; therefore, it determines the starting pressure,  $P_n > P_{eq}$ , of the I<sub>h</sub> → sII transition. The  $P_n$  pressure is indicated by the “sideways perpendicular” symbol in Figure 2a. The nucleation of gas hydrates always starts suddenly and develops in rather a catastrophic manner.<sup>10,13</sup> The volume effect of the I<sub>h</sub> → sII transition is negative at constant  $T$  and  $P$ . Therefore, after the pressure is raised above  $P_n$  to

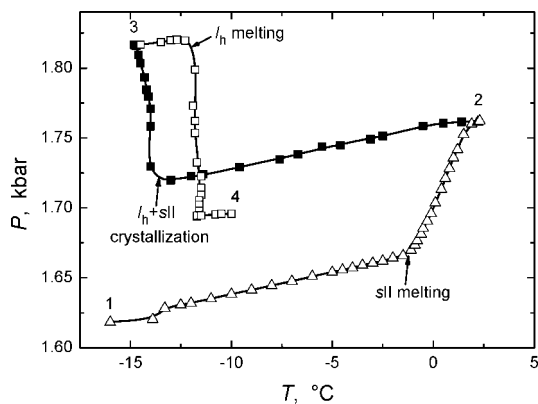


**Figure 3.** Variation of pressure,  $P$ , in the closed autoclave that was heated and cooled in the succession of 1 to 4. The arrows show the transition points indicated in Figure 1.

initiate the  $I_h \rightarrow sII$  transition and we fix the volume of the system, the pressure suddenly begins decreasing. The formation of new stable nuclei of the  $sII$  phase stops when the pressure decreases to  $P_n$ , and the growth of the existing nuclei also stops when the pressure drops below  $P_g$ . To further increase the degree of the  $I_h \rightarrow sII$  conversion, the pressure should be raised again, but not necessarily above  $P_n$ , as the transition could proceed via the growth of the existing numerous nuclei of the  $sII$  phase alone, without the creation of new nuclei. The process stops again, when the pressure decreases to  $P_g$ , and the cycle should be repeated until most ice  $I_h$  transforms to the clathrate phase. The  $P_g$  pressure could noticeably decrease in every cycle due to the increasing size of the growing  $sII$  particles and the concomitant decrease in the contribution of their surface energy to the energy balance. To better localize the equilibrium pressure in the  $T$ - $P$  diagram of Figure 1, we considered the minimum  $P_g$  pressure of the resulting S-shaped  $X(P)$  dependence (solid circle in Figure 2a) as the pressure of the  $I_h \rightarrow sII$  transition.

In the course of the reverse  $sII \rightarrow I_h$  transition, we had  $P_n < P_g < P_{eq}$ , so the maximum  $P_g$  pressure of the S-shaped concentration dependence (open circle in Figure 2a) was considered as the transition pressure. As seen from Figure 1, the temperature dependences of the points of the  $I_h \rightarrow sII$  and  $sII \rightarrow I_h$  transitions can be represented by thin straight lines drawn, correspondingly, through the solid and open circles. These lines are rather close to each other and leave little freedom in drawing the equilibrium line that should lie somewhere between them. We plotted the equilibrium line in the middle. The slope of this thick, solid line in Figure 1 is positive and is equal to 128(10) K/kbar.

**The  $I_h \leftrightarrow L$  and  $sII \leftrightarrow L$  Transformations.** Typical isochors used to determine the melting and crystallization points of the  $I_h$  and  $sII$  phases are shown in Figure 3. We always started with heating a powdered sample of nearly pure  $sII$  phase (point 1 in Figure 3). The melting of the  $sII$  phase was accompanied by a rather steep increase in pressure. The cooling of the melted sample (route 2  $\rightarrow$  3) also led to a phase transition, causing a steep increase in pressure. On subsequent heating (route 3  $\rightarrow$  4), the sample underwent a phase transition that resulted in a pressure decrease and occurred at a temperature much lower than the melting temperature of the  $sII$  phase.

There is only one form of water ice that melts with a negative volume effect. This is ice  $I_h$ , and the phase transitions observed on cooling and further heating the melted  $sII$  sample were located close to the melting curve of ice  $I_h$  in the absence of deuterium gas,<sup>8</sup> which is shown by the dashed curve in Figure 1. This suggests that a considerable part of the liquid should

have transformed to the metastable  $I_h$  phase instead of the stable  $sII$  phase. As one can see from Figure 1, all experimental melting points of the  $I_h$  phase (open squares) can be approximated with a single smooth curve that is plotted thick in the stable region of this phase and thin in the metastable region, beyond the triple point.

Another test of the self-consistency of the proposed interpretation is that according to the phase rule, the equilibrium melting of ice  $I_h$  under isochoric conditions should occur within a finite temperature interval, and the resulting portion of the  $T$ - $P$  dependence should fall onto the line of the  $I_h \leftrightarrow L$  equilibrium in the  $T$ - $P$  diagram. As one can see from Figure 1, this is, in fact, observed because the pairs of connected open squares attributed to the melting intervals of ice  $I_h$  are oriented along the suggested melting curve.

Further experiments showed that the crystallization of ice  $I_h$  in the stability range of the  $sII$  phase was accompanied by the formation of this stable phase. Namely, if the sample was brought to the state indicated by point 4 in Figure 3 and further heated, it showed a steeper increase in pressure in the temperature interval of the  $sII \rightarrow L$  transition. Therefore, it contained some amount of the  $sII$  phase. If the sample was repeatedly cooled and heated across the temperature interval of the  $I_h \leftrightarrow L$  transformation, this reduced the magnitude of the pressure changes accompanying the crystallization and melting of ice  $I_h$ . Therefore, such a cycling decreased the amount of the metastable ice  $I_h$  in the sample and most likely increased the amount of the stable  $sII$  phase. Cooling below the crystallization interval of ice  $I_h$  did not lead to any phase transitions. Taken together, these facts indicate that the  $I_h$  and  $sII$  phases crystallized simultaneously.

The simultaneous crystallization with ice  $I_h$  is typical of most gas clathrate hydrates (see, e.g., ref 14 and references therein). Nevertheless, its mechanism is not well-understood yet, despite the intense experimental and theoretical investigations. It is only established rather reliably that ice  $I_h$  forms first, and its particles serve as nucleation sites for the hydrate.<sup>14</sup>

In the case of the  $D_2O$ - $D_2$  system, the smaller deuterium solubility in ice  $I_h$  than in heavy water can explain why the  $sII$  phase and ice  $I_h$  crystallize together. In fact, the growing particles of ice  $I_h$  should supersaturate the bordering layers of water with the escaping deuterium molecules, thus providing more favorable conditions for the nucleation and growth of the deuterium-rich  $sII$  phase. In its turn, the growing  $sII$  phase depletes the water of the dissolved deuterium molecules, thereby facilitating the nucleation and growth of the deuterium-poor ice  $I_h$ .

The decomposition of gas clathrate hydrates is studied to a much less extent than their formation. A number of researches have reported incomplete or delayed decomposition of these hydrates under conditions such that the hydrate is expected to be unstable and should decompose rapidly (see, e.g., ref 15 and references therein). The decomposition of the hydrogen clathrate hydrate to the liquid and hydrogen gas—the incongruent melting—was earlier described as a very sluggish process that lasts for hours and does not really bring the system to the equilibrium state.<sup>1</sup>

In the intervals of melting of the  $sII$  phase in our isochoric heating experiments (Figure 3), the pressure stopped changing within the experimental error after a 20 min exposure to every given temperature. Figure 1 shows the resulting  $P$ -vs- $T$  paths by arrows connecting the starting (open triangles) and ending (horizontal bars) points of the transitions. As one can see, these arrows do not fall onto a single curve, and therefore, they do not represent the equilibrium melting paths. Because the melting



could not begin at a temperature below the equilibrium one, its starting point should have been most close to the equilibrium conditions. In Figure 1, the sII ↔ L equilibrium is presented by the thick solid line drawn through the starting points of the sII → L transitions.

The lines of the I<sub>h</sub> ↔ sII and I<sub>h</sub> ↔ L equilibria in the *T*–*P* diagram of the D<sub>2</sub>O–D<sub>2</sub> system are determined more accurately and intersect at *P* = 1.07(3) kbar and *T* = –4.5(8) °C. As seen from Figure 1, the sII ↔ L equilibrium line passes through this triple point, too, and has a slope of 6.0(3) K/kbar. The slope of the I<sub>h</sub> ↔ L line near the triple point is –7.8(2) K/kbar.

**The Deuterium Content of the sII, I<sub>h</sub>, and L Phases.** Turning back to Figure 2, one can see that the deuterium concentration of the D<sub>2</sub>O–D<sub>2</sub> samples did not change fully reversibly with increasing and decreasing pressure in the range of stability of the sII phase. The reason was obviously that the formation of the sII phase remained incomplete, even at the maximum pressure of ~1.9 kbar. Earlier,<sup>5</sup> a D<sub>2</sub>O–D<sub>2</sub> sample of the sII phase prepared under a deuterium pressure of 1.7 kbar and temperature –20 °C in the same manner as the samples in the present work was examined by neutron diffraction and shown to contain ~1% unreacted ice I<sub>h</sub>. Most likely, our samples loaded with deuterium at 1.9 kbar while constructing the isotherms at increasing pressure contained a similar amount of ice I<sub>h</sub>. Each isotherm measured at the pressure decreasing from 1.9 kbar to the point of the sII → I<sub>h</sub> transition could therefore give the deuterium content of the sII phase underestimated by ~1%. We neglected this possible systematic error because the absolute accuracy of the measurement was ~2%.

The concentrations  $X_{sII}^{calc}$  and  $X_{Ih}^{calc}$  of the sII and I<sub>h</sub> phases along the equilibrium line,  $P_{eq}(T)$ , of the I<sub>h</sub> ↔ sII transformation (thick, solid line in Figure 1) were determined as the  $X(P_{eq})$  values in the isotherms measured at decreasing and increasing pressure, respectively (see Figure 2). Within the experimental error, neither concentration changed in the studied temperature interval –40 to –10 °C, and their mean values were  $X_{sII}^{calc} = 0.207(5)$  and  $X_{Ih}^{calc} = 0.015(5)$ . One should expect that these concentrations were the same at the L + I<sub>h</sub> + sII triple point located nearby at –4.5 °C. The deuterium concentration,  $X_L = 0.025(8)$ , of the liquid near the triple point was determined less accurately in an individual experiment. The difference  $X_L - X_{Ih} = 0.008(4)$  also determined in this experiment is consistent with the estimated value of  $X_{Ih} = 0.015(5)$ .

The triple point is traditionally an object for testing the integrity and consistency of experimental data because a number of different conditions must be met simultaneously at the triple points. Namely, the independently determined equilibrium lines of three transformations must pass through a common point, which is satisfied in our case. The three independently determined changes in volume,  $\Delta V_i$ , accompanying these transformations must answer the additive relation, which is also satisfied because we directly measured the volumes of each of the three equilibrium states of the system. Finally, the three changes in entropy,  $\Delta S_i$ , must answer the additive relation, too, and this connects  $\Delta V_i$  and the slopes  $(dT/dP)_i$  of the transformation lines via Clapeyron's equation so that

$$\sum \Delta S_i = \sum (dT/dP)_i / \Delta V_i = 0 \quad (1)$$

We used eq 1 to independently estimate the  $X_{Ih}$  and  $X_L$  values at the triple point of the D<sub>2</sub>O–D<sub>2</sub> system, assuming that  $X_{Ih}/X_L = 0.64$ . This ratio was experimentally determined for the I<sub>h</sub> and L phases in the H<sub>2</sub>O–H<sub>2</sub> system at 0.3 kbar and 0 °C.<sup>16</sup> It agrees with a value of  $X_{Ih}/X_L = 0.011/0.017 \approx 0.6$  at the triple point (1.07 kbar, –10 °C) of the H<sub>2</sub>O–H<sub>2</sub> system<sup>4</sup> and is likely to

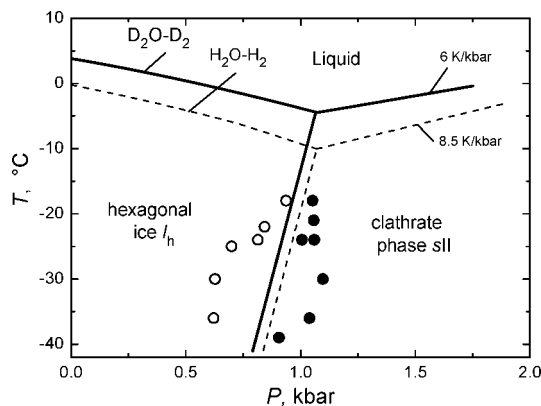


**Figure 4.** *T*–*P* diagram of phase equilibria in the D<sub>2</sub>O–D<sub>2</sub> system (solid lines) and H<sub>2</sub>O–H<sub>2</sub> system (dashed lines, results of ref 4). Closed and open circles show the points of the I<sub>h</sub> → sII and sII → I<sub>h</sub> phase transitions, respectively, in the H<sub>2</sub>O–H<sub>2</sub> system.<sup>4</sup> The I<sub>h</sub> ↔ sII equilibrium line in the H<sub>2</sub>O–H<sub>2</sub> system is plotted with the same slope,  $dT/dP = 128$  K/kbar, as in the D<sub>2</sub>O–D<sub>2</sub> system.

hold for the I<sub>h</sub> and L phases in the D<sub>2</sub>O–D<sub>2</sub> system, too, under similar conditions. Using  $X_{Ih} = 0.64X_L$  and solving eq 1 for  $X_L$  with all other parameters taken from experiment gives  $X_{Ih}^{calc} = 0.012$  and  $X_L^{calc} = 0.020$  for the L + I<sub>h</sub> + sII triple point of D<sub>2</sub>O–D<sub>2</sub>. These values agree with the experimental  $X_{Ih} = 0.015(5)$  and  $X_L = 0.025(8)$ . Moreover, we consider the calculated values more reliable and accurate because they are fully consistent with the whole set of other parameters characterizing the D<sub>2</sub>O–D<sub>2</sub> phases at the triple point.

We also used eq 1 to slightly reduce the uncertainty in the parameters of the triple point in the H<sub>2</sub>O–H<sub>2</sub> system examined earlier.<sup>4</sup>

The points of the I<sub>h</sub> → sII and sII → I<sub>h</sub> transitions in the H<sub>2</sub>O–H<sub>2</sub> system (Figure 4) show a larger scatter and hysteresis than in the D<sub>2</sub>O–D<sub>2</sub> system (Figure 1), which makes the slope of the I<sub>h</sub> ↔ sII equilibrium line less definite. Assuming that the slope of this line is the same as in the D<sub>2</sub>O–D<sub>2</sub> system and solving eq 1 for  $X_{sII}$  with all other parameters taken from experiment gives  $X_{sII}^{calc} = 0.207$  at the triple point of H<sub>2</sub>O–H<sub>2</sub>. The calculated value agrees with  $X_{sII} = 0.212(9)$  measured in ref 4 and coincides with the experimental value of  $X_{sII} = 0.207(5)$  at the triple point of the D<sub>2</sub>O–D<sub>2</sub> system determined in the present paper. Similar compositions of phases at the triple points of the H<sub>2</sub>O–H<sub>2</sub> and D<sub>2</sub>O–D<sub>2</sub> systems are very likely, so the calculation corroborates the assumption that the slopes of the I<sub>h</sub> ↔ sII equilibrium lines in these systems are similar, too.

The most feasible values of thermodynamic parameters of the phases and phase transformations near the triple points in the D<sub>2</sub>O–D<sub>2</sub> and H<sub>2</sub>O–H<sub>2</sub> systems are collected in Tables 1 and 2. The third column of Table 1 presents the total change in volume ( $\Delta V$ ) accompanying the phase transition. This volume change can be written as the sum  $\Delta V = \Delta V_{cond} + \Delta V_{gas}$  of volume changes of the condensed phases (last column of Table 1) and the gaseous phase.

**Thermal and Concentration Stability of the sII Phase.** In the cubic unit cell of the sII phase formed by 136 D<sub>2</sub>O molecules, there are two types of cages accessible to guest molecules: 8 “large” and 16 “small” ones. The in situ neutron diffraction investigation<sup>3</sup> showed that the large and small cages can accommodate up to four and one D<sub>2</sub> molecule, respectively, which corresponds to  $X_{sII}^{max} = 48/136 \approx 0.353$ . The deuterium content of the sII phase and the occupancies of cages of both types vary with pressure and temperature. The distribution of

**TABLE 1: Parameters of Phase Transformations near the Triple Point of the L + I<sub>h</sub> + sII Equilibrium in the D<sub>2</sub>O–D<sub>2</sub> System ( $P = 1.07$  kbar,  $T = -4.5$  °C) and H<sub>2</sub>O–H<sub>2</sub> System ( $P = 1.07$  kbar,  $T = -10$  °C)<sup>a</sup>**

system	transition	$\Delta V$ , cm <sup>3</sup> /mol	$dT/dP$ , K/kbar	$\Delta S$ , J/K/mol	$\Delta H$ , kJ/mol	$\Delta V_{\text{cond}}$ , cm <sup>3</sup> /mol
D <sub>2</sub> O–D <sub>2</sub>	I <sub>h</sub> → sII	−4.42	128	−3.45	−0.93	2.67
	sII → L	2.04	6.0	34.0	9.13	−4.80
	L → I <sub>h</sub>	2.38	−7.8	−30.5	−8.19	2.12
H <sub>2</sub> O–H <sub>2</sub>	I <sub>h</sub> → sII	−4.33	128	−3.38	−0.89	2.80
	sII → L	2.05	8.5	24.1	6.34	−4.85
	L → I <sub>h</sub>	2.28	−11.0	−20.7	−5.44	2.05

<sup>a</sup> The changes in volume ( $\Delta V$ ), entropy ( $\Delta S$ ), enthalpy ( $\Delta H$ ), and volume of the condensed phases ( $\Delta V_{\text{cond}}$ ) are calculated per 1 gram–mol of D<sub>2</sub>O and H<sub>2</sub>O, respectively.

**TABLE 2: Molar Ratio ( $X$ ) and Molar Volume ( $V$ ) of Condensed Phases at the Triple Point of the L + I<sub>h</sub> + sII Equilibrium in the D<sub>2</sub>O–D<sub>2</sub> and H<sub>2</sub>O–H<sub>2</sub> Systems**

phase	D <sub>2</sub> O–D <sub>2</sub>		H <sub>2</sub> O–H <sub>2</sub>	
	$X = \text{D}_2/\text{D}_2\text{O}$	$V$ , cm <sup>3</sup> /mol	$X = \text{H}_2/\text{H}_2\text{O}$	$V$ , cm <sup>3</sup> /mol
I <sub>h</sub>	0.012	19.53	0.011	19.36
L	0.020	17.40	0.017	17.31
sII	0.207	22.20	0.207	22.16

D<sub>2</sub> molecules over the cages as a function of decreasing deuterium content was examined by neutron diffraction for quenched samples of the sII phase heated at ambient pressure.<sup>3,4</sup> A slow heating of the sII sample with the initial  $X \approx X_{\text{sII}}^{\text{max}}$  resulted in a gradual decrease of  $X$  from 48/136 to 32/136  $\approx 0.235$  at temperatures 70–163 K due to the decrease in the occupancy of the large cages from four to two D<sub>2</sub> molecules, the occupancy of the small cages remaining close to one D<sub>2</sub> molecule.<sup>3</sup> On heating above 163 K, the sII phase collapsed. In another work,<sup>4</sup> an sII sample with  $X \approx 32/136$  was studied at 95 K in the as-prepared state and after successive runs of rapid heating to a chosen temperature, annealing at that temperature for 15 min and rapid cooling back to 95 K. The initial sample contained, respectively, two and one D<sub>2</sub> molecule in every large and small cage, in agreement with results of ref 3. After annealing at 195 K, the occupancy of the small cages decreased to  $\sim 0.7$  D<sub>2</sub> molecule. After further annealing at 220 K, about half of the sample transformed to a mixture of D<sub>2</sub>O phases without deuterium, but the distribution of the deuterium molecules in the remaining sII phase did not change.

The latter result suggests that 2 D<sub>2</sub> molecules in the large cage and 0.7 D<sub>2</sub> molecules in the small cage are the lowest occupancies required for the stability of the sII phase of D<sub>2</sub>O–D<sub>2</sub> at ambient pressure. This deuterium distribution gives  $X_{\text{sII}}^{\text{min}} \approx 0.200$ . Interestingly, it is exactly the composition of the sII phase at which the sII → I<sub>h</sub> transition began in our high-pressure experiments (see Figure 2). We can therefore conclude that even at submelting temperatures of the sII and I<sub>h</sub> phases, the sII phase starts transforming to ice I<sub>h</sub> only when it loses its thermodynamic stability. The thin dashed curve in Figure 5 shows the low-pressure boundary of the  $T$ – $P$  region where the sII phase can exist. Along this curve, the deuterium content of the sII phase is close to  $X_{\text{sII}}^{\text{min}} \approx 0.200$ .

The deuterium content of the sII phase in equilibrium with the I<sub>h</sub> phase along the I<sub>h</sub> ↔ sII line and in the triple point is close to  $X = 0.207$ . Most likely, the distribution of D<sub>2</sub> molecules in the clathrate structure of this phase is the same as in the metastable sII phase with  $X \leq 0.235$  studied by neutron diffraction at ambient pressure;<sup>4</sup> namely, every large cage encloses two D<sub>2</sub> molecules, and the remaining D<sub>2</sub> molecules randomly occupy the small cages; in our case, with a probability of 0.76.

The close similarity between the phase diagrams and practically coinciding  $X \approx 0.207$  of the sII phase at the triple points

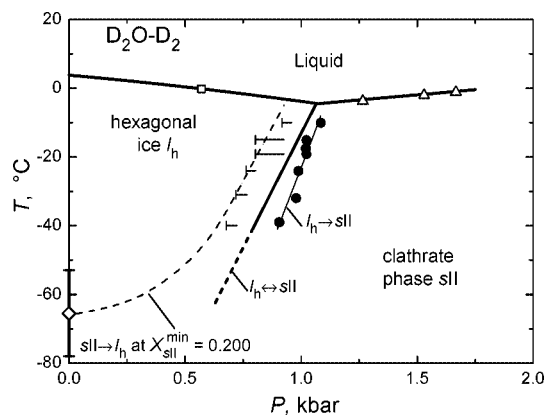


**Figure 5.**  $T$ – $P$  diagram of the D<sub>2</sub>O–D<sub>2</sub> system. The thin dashed curve is drawn through the starting points of decomposition of the sII phase at decreasing pressure (“sideways perpendicular”; data of the present work) and increasing temperature (open diamond; data from ref 4).

in the D<sub>2</sub>O–D<sub>2</sub> and H<sub>2</sub>O–H<sub>2</sub> systems suggest the similarity between the concentration dependences of the distribution of guest molecules in the clathrate framework of this phase. In particular, one can expect the occupancies of 2 and 0.76 H<sub>2</sub> molecules, respectively, of the large and small cages in the sII phase at the triple point of the H<sub>2</sub>O–H<sub>2</sub> system.

The thermal stability of the D<sub>2</sub>O–D<sub>2</sub> and H<sub>2</sub>O–H<sub>2</sub> clathrate sII phases at ambient pressure cannot be directly compared because this is not an equilibrium thermodynamic property; therefore, it depends on the experimental procedure used. Nevertheless, the H<sub>2</sub>O–H<sub>2</sub> phase is likely to be less stable because its decomposition was observed at 140–145 K,<sup>2,10</sup> whereas in ref 3, the D<sub>2</sub>O–D<sub>2</sub> phase was reported to decompose at 163 K, and in ref 4, it still existed in a sample heated to 220 K.

## Conclusions

The  $T$ – $P$  diagram of the D<sub>2</sub>O–D<sub>2</sub> system is similar to that of the H<sub>2</sub>O–H<sub>2</sub> system studied earlier.<sup>1,4,6</sup> In particular, the triple point of the L + I<sub>h</sub> + sII equilibrium is located at the same pressure of 1.07 kbar, and its temperature is raised by only 5.5 °C. The D<sub>2</sub>/D<sub>2</sub>O and H<sub>2</sub>/H<sub>2</sub>O molar ratios ( $X$ ) for each phase at the triple point are also similar. The value of  $X = 0.207(5)$  established for the sII phase at the triple point in both systems implies the occupancies of the large and small cages in its clathrate structure by 2 and 0.76 D<sub>2</sub> (H<sub>2</sub>) molecules, respectively.

Phase transitions involving the sII phase are very sluggish. Two new features of these transitions are revealed in the present work. First, the sII → I<sub>h</sub> transition at decreasing pressure starts no earlier when the deuterium content of the sII phase decreases to the minimum value of  $X \approx 0.200$  necessary for its stability. Second, the formation of the sII phase from the liquid at decreasing temperature can only occur together with the formation of a metastable phase of ice I<sub>h</sub>.

The simultaneous crystallization of ice I<sub>h</sub> and clathrate on supercooling is typical of many water–gas and water–fluid systems. In the D<sub>2</sub>O–D<sub>2</sub> system, this phenomenon can be explained by the smaller deuterium solubility in ice I<sub>h</sub> than in heavy water. Namely, the growing particles of ice I<sub>h</sub> should supersaturate the surrounding of water with deuterium, thus providing more favorable conditions for the nucleation and growth of the deuterium-rich sII phase. In its turn, the growing sII phase depletes the water of the dissolved deuterium, therefore facilitating the nucleation and growth of the deuterium-poor ice, I<sub>h</sub>.

**Acknowledgment.** This work was supported by the Russian Academy of Sciences (the program “Physics and Mechanics of Strongly Compressed Matter”), the Russian Foundation for Basic Research (Grant no. 05-02-17733) and the Foundation for Support of Russian Science.

### References and Notes

- (1) Dyadin Yu., A.; Larionov, E. G.; Manakov, A. Yu.; Zhurko, F. V.; Aladko, E. Ya.; Mikina, T. V.; Komarov, V. Yu. *Mendeleev Commun.* **1999**, 209–210.
- (2) Mao, W. L.; Mao, H.-K.; Goncharov, A. F.; Struzhkin, V. V.; Guo, Q.; Hu, J.; Shu, J.; Hemley, R. J.; Somayazulu, M.; Zhao, Y. *Science* **2002**, 297, 2247–2249.
- (3) Lokshin, K. A.; Zhao, Y.; He, D.; Mao, W. L.; Mao, H.-K.; Hemley, R. J.; Lobanov, M. V.; Greenblatt, M. *Phys. Rev. Lett.* **2004**, 93, 125503-1–125503-4.
- (4) Efimchenko, V. S.; Antonov, V. E.; Barkalov, O. I.; Beskrovnyy, A. I.; Fedotov, V. K.; Klyamkin, S. N. *High Pressure Res.* **2006**, 26, 439–443.
- (5) Lokshin, K. A.; Zhao, Y. *Appl. Phys. Lett.* **2006**, 88, 131909-1–131909-3.
- (6) Barkalov, O. I.; Klyamkin, S. N.; Antonov, V. E.; Efimchenko, V. S. *JETP Lett.* **2005**, 82, 413–415.
- (7) Klyamkin, S. N.; Verbetsky, V. N. *J. Alloys Compd.* **1993**, 194, 41–45.
- (8) Bridgman, W. B. *J. Chem. Phys.* **1935**, 3, 597–605.
- (9) Tkacz, M.; Litwiniuk, A. *J. Alloys Compd.* **2002**, 330–332, 89–92.
- (10) Mao, W. L.; Mao, H.-K. *Proc. Nat. Acad. Sci. U.S.A.* **2004**, 101, 708–710.
- (11) Tiepel, E. W.; Gubbins, K. E. *J. Phys. Chem.* **1972**, 76, 3044–3049.
- (12) Moore, J. C.; Battino, R.; Rettich, T. R.; Handa, Y. P.; Wilhelm, E. *J. Chem. Eng. Data* **1982**, 27, 22–24.
- (13) Bishnoi, P. R.; Natarjan, V. *Fluid Phase Equilib.* **1996**, 117, 168–177.
- (14) Zhang, Y.; Debenedetti, P. G.; Prud’homme, R. K.; Pethica, B. A. *J. Phys. Chem. B* **2004**, 108, 16717–16722.
- (15) Wilder, J. W.; Smith, D. H. *J. Phys. Chem. B* **2002**, 106, 6298–6302.
- (16) Namiot, A. Yu.; Bukhgalter, E. B. *Zh. Strukt. Khim.* **1965**, 6, 911–912. , *J. Struct. Chem. (Engl. Transl.)* **1965**, 6, 873–874.

JP800487Y